Title

14C evidence that millennial and fast-cycling soil carbon are equally sensitive to warming

Journal

Nature Climate Change, 9(6)

ISSN

1758-678X

Authors

Vaughn, Lydia JS
Torn, Margaret S

Publication Date

2019-06-01

DOI

10.1038/s41558-019-0468-y

Peer reviewed

^{14}C evidence that millennial and fast-cycling soil carbon are equally sensitive to warming

Lydia J. S. Vaughn[1,2]* and Margaret S. Torn[1,3]*

[1] Lawrence Berkeley National Laboratory, Berkeley, CA, USA. [2] Integrative Biology, University of California, Berkeley, Berkeley, CA, USA. [3] Energy and Resources Group, University of California, Berkeley, Berkeley, CA, USA. *e-mail: lydiajsmith@lbl.gov; mstorn@lbl.gov

Abstract

The Arctic is expected to shift from a sink to a source of atmospheric CO_2 this century due to climate-induced increases in soil carbon mineralization[1]. The magnitude of this effect remains uncertain, largely because temperature sensitivities of organic matter decomposition[2,3] and the distribution of these temperature sensitivities across soil carbon pools[4] are not well understood. Here, a new analytical method with natural abundance radiocarbon was used to evaluate temperature sensitivities across soil carbon pools. With soils from Utqiaġvik (formerly Barrow), Alaska, an incubation experiment was used to evaluate soil carbon age and decomposability, disentangle the effects of temperature and substrate depletion on carbon mineralization, and compare temperature sensitivities of fast-cycling and slow-cycling carbon. Old, historically stable carbon was shown to be vulnerable to decomposition under warming. Using radiocarbon to differentiate between slow-cycling and fast-cycling carbon, temperature sensitivity was found to be invariant among pools, with a Q_{10} of ~2 irrespective of native decomposition rate. These findings suggest that mechanisms other than chemical recalcitrance mediate the effect of warming on soil carbon mineralization.

Main

High-latitude soils are an important carbon reservoir. Cold, frozen and anoxic conditions have stabilized soil organic matter, leading to the accumulation of an estimated 1,300 Pg of carbon, nearly equal to that stored in global vegetation and the atmosphere combined[5]. Over the coming decades, the Arctic is expected to shift from a sink to a source of atmospheric CO_2 as soil warming and permafrost thaw destabilize this carbon[1,6]. Such changes have already been seen. Research has documented rising soil temperatures and permafrost thaw[7,8], with increased rates of soil carbon mineralization, particularly from old, previously stable pools[9,10].

Model predictions of high-latitude soil carbon losses range widely, from 37 to 174 Pg by 2100 for equivalent anthropogenic emissions scenarios[6]. Model sensitivities underlying this range include the parameterized, nominal soil carbon decomposability[3] and the temperature sensitivity of carbon mineralization[2,11]. Soil organic matter is a heterogeneous mixture with a range of chemical compositions, cycling rates and stabilization mechanisms. As such, soil carbon vulnerabilities to climate change depend on the

distribution of organic compounds, their physio-chemical states, microbial activity and environmental context. To describe dynamics of this heterogeneous system, bulk soil carbon can be partitioned into pools, defined operationally by their decomposition rates[2,12]. These decomposition rates are functions of chemical recalcitrance, physical and chemical protection in the soil matrix and environmental variables such as temperature and oxygen availability[2,13].

Despite more than a decade of research on soil fractions and decomposition dynamics, no consensus has been reached about how temperature sensitivities vary across soil carbon pools[14]. Kinetic theory predicts that decomposition of compounds with higher activation energies (greater chemical stability) should be more sensitive to temperature changes than more chemically labile substrates[2]. If the cycling rate of soil organic matter depends on its chemistry, theory predicts that slow-cycling carbon will be particularly vulnerable to warming. Numerous studies have used incubation and field experiments to test this prediction, with varied and often inconclusive results[14]. Some have found that slow-cycling, less decomposable carbon pools are more responsive to temperature changes[4,15,16,17]. Others have found that carbon pools have neither different temperature sensitivities[18,19,20,21] nor distinct chemical compositions[22], challenging simple relationships between carbon cycling rate, substrate chemistry and temperature sensitivity.

A common approach such studies use is to measure CO_2 production under separate temperature treatments and estimate temperature sensitivities of different source pools by fitting multi-pool models with Arrhenius-type kinetics to CO_2 emissions. Several challenges inherent to this approach may lead to erroneous conclusions. Without a clear tracer differentiating carbon pools, bulk CO_2 flux measurements alone usually provide insufficient information to falsify or effectively parameterize models[23], leaving results sensitive to assumptions and predetermined model characteristics such as functional form and number of pools. In non-steady-state incubations, temperature sensitivities may be difficult to disentangle from microbial community changes and thermal adaptation[24]. Statistical effects may confound relationships among respiration rates and temperature sensitivities[23]. Finally, incubations introduce experimental artifacts. The common practice of soil homogenization, for instance, destabilizes carbon by disrupting soil aggregates[13], altering relationships between chemistry and decomposability.

To address such challenges, we developed a new methodology with natural abundance radiocarbon to evaluate the temperature sensitivities of fast-cycling and slow-cycling soil carbon in an Arctic tundra ecosystem. A naturally occurring tracer of carbon dynamics, radiocarbon in CO_2 reflects the age of respired carbon[12], enabling us to estimate carbon dynamics metrics from individual measurements without having to fit models to CO_2 fluxes. Additionally, radiocarbon offers information on very slow-cycling

carbon pools that CO_2 production rates alone may not capture in the timeframe of incubation studies.

With soils from Utqiaġvik, Alaska, we incubated intact (non-homogenized) soil samples at 5 °C and 10 °C, a realistic summertime temperature range for near-surface soils. Using CO_2 production and its radiocarbon abundance ($\Delta^{14}C_{CO_2}$), we estimated historical cycling rates of respired carbon and isolated active-pool and passive-pool temperature sensitivities. Rather than homogenize soils to generate experimental units, we performed sequential incubations with intact samples at 5 °C and 10 °C. By allowing the use of intact soil samples, this approach minimized soil disturbance, preserving physical carbon stabilization mechanisms[13] whose temperature sensitivities may differ from kinetic predictions[14,25]. A consideration of this design, however, is that depletion of labile substrates alters CO_2 production and $\Delta^{14}C_{CO_2}$ between sequential incubations. To correct for these effects, we performed a third incubation at the baseline temperature of 5 °C.

$\Delta^{14}C_{CO_2}$ from the first incubation ranged from +86.5‰ to −48.3‰ in near-surface samples and from −72.3‰ to −326.4‰ near the permafrost table (Table 1). Positive $\Delta^{14}C_{CO_2}$ values indicate high percentages of carbon fixed since 1960, whereas highly negative values reflect large proportions of carbon that cycles on centennial to millennial timescales. To estimate cycling rates, we used $\Delta^{14}C_{CO_2}$ measurements in a time-dependent, steady-state model to calculate ages of carbon undergoing mineralization. (Age, a characteristic time constant for soil carbon dynamics, equals turnover time for well-mixed, steady-state systems.) Carbon ages ranged broadly, from ~100 to 700 yr in shallow samples and from ~1,500 to 4,200 yr at depth (Table 1). These strong vertical gradients in $\Delta^{14}C_{CO_2}$ and CO_2 age demonstrate shifts from fast-cycling carbon near the soil surface to more slow-cycling carbon at depth. This depth trend is common at high latitudes, where cold temperatures and short thaw seasons generate steep vertical gradients in decomposition rates[10,26]. However, our $\Delta^{14}C_{CO_2}$ values were nearly an order of magnitude lower at similar depths compared to those studies; at only ~15–30 cm, we observed decomposition of carbon that cycles on millennial timescales. Co-located field-based measurements of $\Delta^{14}C_{CO_2}$ in soil surface emissions and soil pore-space confirm that these incubation results reflect in situ cycling rates[27]. At 20 cm depth, soil pore-space CO_2 ages were as great as ~3,000 yr (median = 1,375 yr). In both

incubations and in situ soils, we thus see that ancient soil carbon is readily decomposable under unfrozen, aerobic conditions.

Table 1 | Isotopic composition and age of CO_2 released during the first (5 °C) incubation

Soil core	Depth (cm)	$\delta^{13}C_{CO2}$ (‰)	$F^{14}C$	$\Delta^{14}C_{CO_2}$ (‰)	Carbon age (yr)
Core 1	0–14	−29.4	1.033	25.2 ± 3.1	260[a]
	14–31	-	0.7899[b]	−216.1 ± 3.0[b]	2,440
Core 2	0–7	−27.9	1.0415	33.6 ± 3.5	<3 or 230
	7–27	−22.7	0.9640	−43.3 ± 3.6	640
	27–37	−25.3	0.9348	−72.3 ± 3.0	870
Core 3	0–13	−26.4	0.9914	−16.1 ± 2.9	460
	13–27	−26.7	0.7976	−208.5 ± 2.5	2,340
Core 4	0–8	−28.1	1.0317	23.8 ± 3.6	<1 or 270
	8–26	−27.2	0.9660	−41.4 ± 2.9	630
	26–39	−22.9	0.7915	−214.6 ± 2.4	2,420
Core 5	0–6	−27.0	1.0675	59.4 ± 3.4	3–8 or 160–170
	11–33	−28.2	0.6787	−326.4 ± 2.5	4,160
Core 6	0–6	−27.7	1.0451	37.2 ± 5.4	<4 or 220
	6–20	−26.8	0.8244	−181.9 ± 2.5	2,000
	20–34	−24.4	0.7181	−287.4 ± 2.4	3,490
Core 7	0–5	−27.3	1.0948	86.5 ± 3.5	7–10 or 110–120
	5–14	−26.8	0.8620	−144.5 ± 4.4	1,570
	14–21	−25.0	0.7989	−207.1 ± 3.6	2,320
Core 8	0–14	−28.7	1.0263	18.6 ± 3.0	290
	14–30	−27.9	0.8468	−141.8 ± 2.8	1,540
Core 9	0–14	−27.7	0.9589	−48.3 ± 3.7	680
	14–35	−27.5	0.7147	−290.7 ± 2.3	3,540

Additional soils information is provided in the Supplementary Information. All radiocarbon analyses were performed at the Lawrence Livermore National Laboratory Center for Accelerator Mass Spectrometry in 2013. Carbon ages reflect the pool of carbon that is being decomposed, that is, the age of carbon in the respiration flux. [a]Alternate carbon age solution of <3 yr was discarded on the basis of values from incubations 2 and 3 (690 and 730 yr). [b]Calculated with an estimated $\delta^{13}C$ value of −25‰.

Between the first two incubations (5 °C and 10 °C), CO_2 production rates increased and $\Delta^{14}C_{CO_2}$ decreased (Fig. 1; Table 2). These changes demonstrate that carbon mineralization responded to the temperature treatment and substrate use shifted toward older soil organic matter. We also observed decreases in both CO_2 production and $\Delta^{14}C_{CO_2}$ between the first and third 5 °C incubations (Fig. 1; Table 2). The changes across incubations in CO_2 production and $\Delta^{14}C_{CO_2}$ varied among samples and were uncorrelated with one another (Supplementary Fig. 1), suggesting that historical cycling rate and decomposability were not consistently related across samples, probably due to inhibition of decomposition by cold, frozen and/or anoxic conditions. Generally, these changes indicate progressive depletion of readily decomposable, fast-cycling substrates, slowing carbon mineralization and increasing relative contributions of slow-cycling carbon to total CO_2 production.

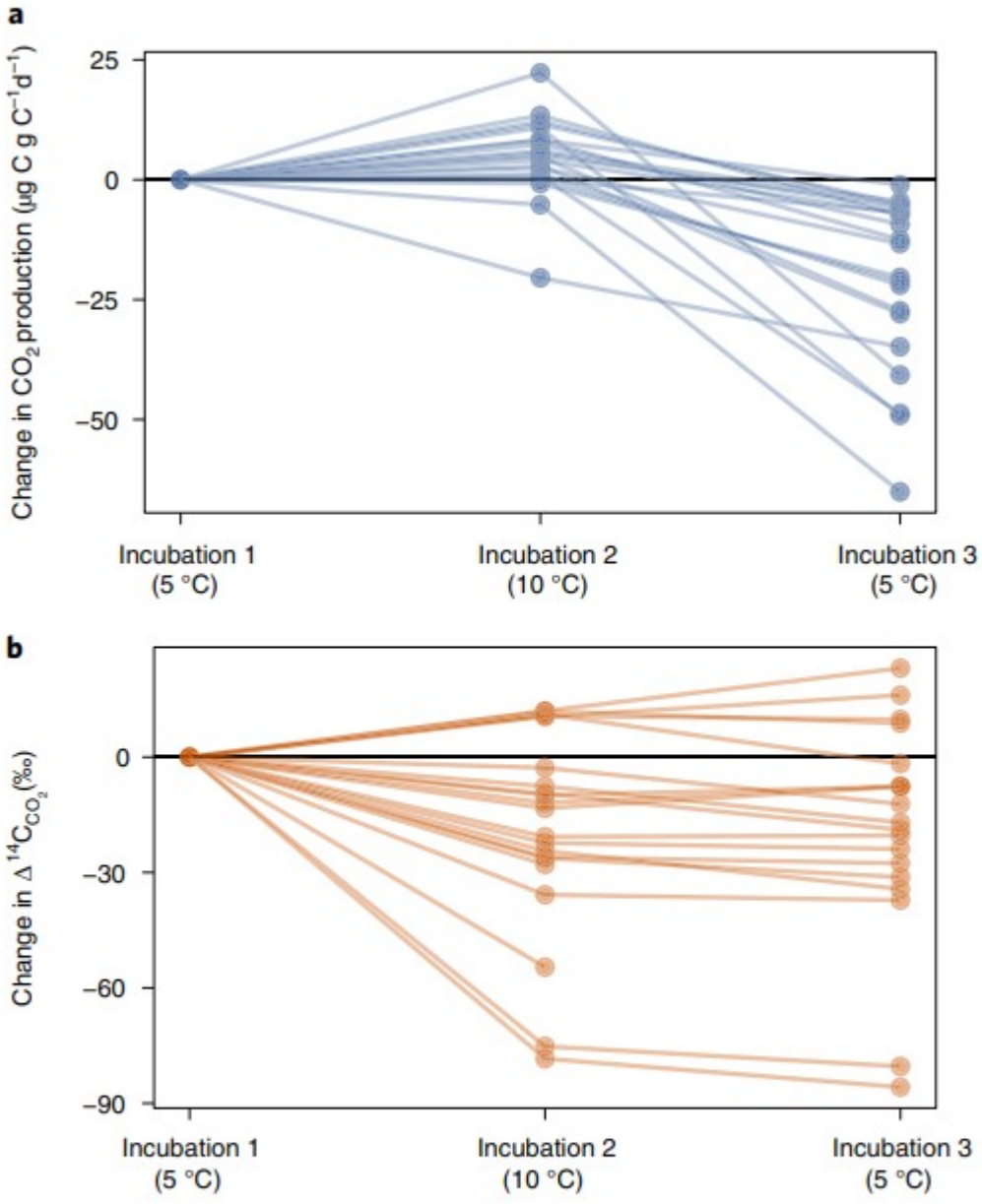

Fig. 1 | Change over time in CO_2 production and $\Delta^{14}C_{CO_2}$ during sequential soil incubations. a,**b**, CO_2 production rates (**a**) and $\Delta^{14}C$ of CO_2 (**b**) are presented as differences relative to the initial 5 °C incubation period. Lines connect measurements from individual soil samples.

Table 2 | Significant predictors from linear mixed-effects models

Response	Coefficient	Estimate	s.e.	d.f.	*t* value	*P* value
$\Delta^{14}C_{CO_2}$ (‰)	Intercept	−98.26	29.81	19.19	−3.30	0.00376
	Incubation 2	−11.28	3.64	35.00	−3.10	0.00379
	Incubation 3	−12.28	3.87	35.01	−3.17	0.00314
CO_2 production ($mg\,C\,g\,C^{-1}\,d^{-1}$; log)	Intercept	−2.92	0.15	20.36	−19.48	<0.00001
	Incubation 2	0.11	0.02	40.00	4.57	0.00005
	Incubation 3	−0.31	0.02	40.00	−12.71	<0.00001
$\Delta_{1,2}$ (%)	Intercept	39.35	2.89	16.33	13.61	<0.00001
	$\Delta_{1,3}$	1.06	0.09	16.83	11.55	<0.00001

Note: Units and transformations used for the response variables are listed in parentheses. Incubation 2 and Incubation 3 are reported relative to Incubation 1. No back-transformation was applied to the coefficients of the model predicting CO_2 production.

To determine the direct, pool-specific temperature sensitivities of CO_2 production, we were required to correct for the background effects of substrate depletion on CO_2 production and $\Delta^{14}C_{CO_2}$. To perform this correction, we defined two metrics for each incubated soil. The first metric, $\Delta_{1,3}$, was calculated as the percentage change in the CO_2 production rate between incubations 1 and 3, both at 5 °C. Metric $\Delta_{1,3}$ thus quantifies the effect of substrate depletion on carbon mineralization. The second metric, $\Delta_{1,2}$, was calculated as the percentage change in CO_2 production between incubations 1 and 2, at 5 °C and 10 °C. Metric $\Delta_{1,2}$ thus quantifies the change in carbon mineralization due to the combined effects of temperature and substrate depletion. Regressing $\Delta_{1,2}$ against $\Delta_{1,3}$, we observed a strong positive linear relationship (Fig. 2; Table 2), which allowed us to estimate temperature sensitivity in the absence of substrate depletion. Specifically, the y-intercept of this regression (39.3 ± 2.8) estimates the percentage change in CO_2 production due to a 5 °C temperature increase if there were no background change in carbon mineralization, that is, when $\Delta_{1,3} = 0\%$. This derived temperature sensitivity corresponds to a Q_{10} of 1.94 ± 0.078, supporting the widespread use of $Q_{10} = 2$ in carbon cycle models[28].

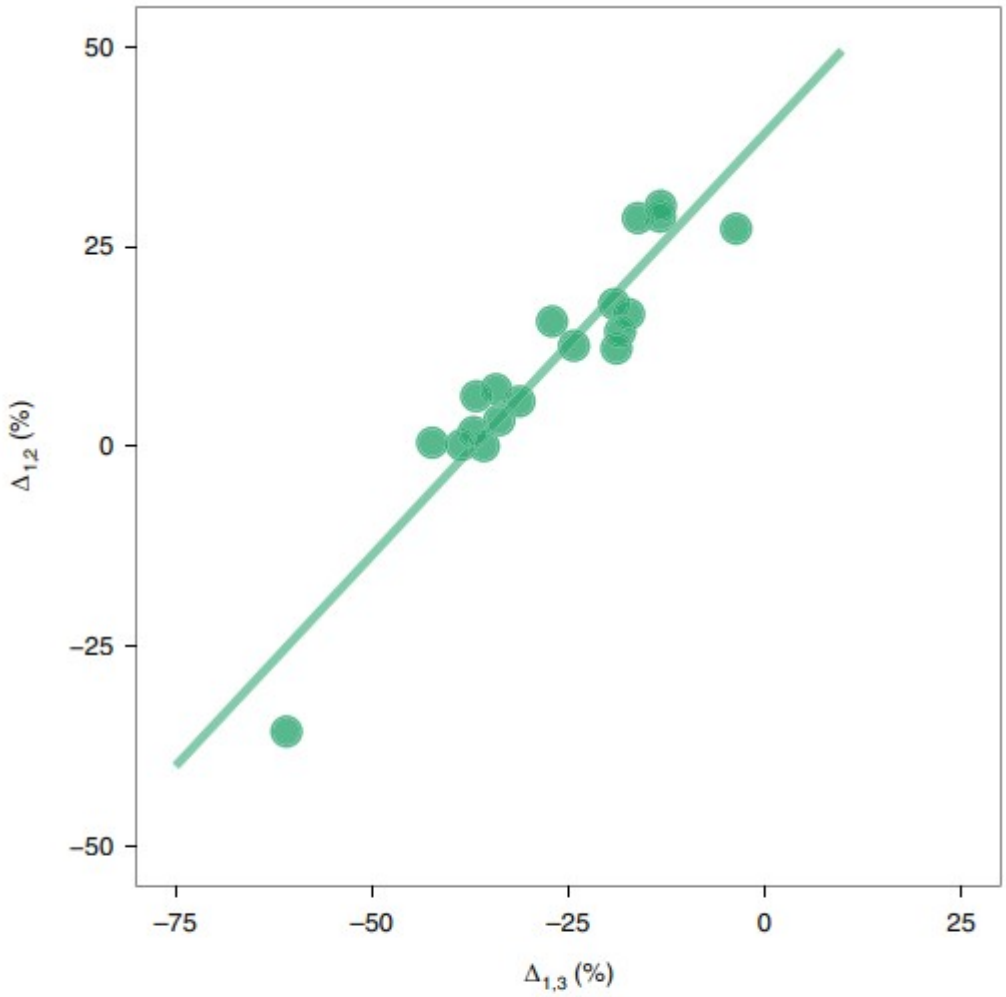

Fig. 2 | Effects of temperature and incubation time on CO_2 production rate. For each incubated soil sample, $\Delta_{1,2}$ is the percentage change in CO_2 production between incubations 1 (5 °C) and 2 (10 °C), and $\Delta_{1,3}$ is the percentage change in CO_2 production between incubations 1 and 3 (both 5 °C). Regression line represents the best linear fit and *y*-intercept (39.3 ± 2.9) estimates the change in CO_2 production due to a 5 °C temperature increase in the absence of any temperature-independent change in the carbon mineralization rate.

To test whether temperature sensitivity differed between fast-cycling and slow-cycling carbon, we incorporated $\Delta^{14}C_{CO_2}$ measurements into the regression between $\Delta_{1,2}$ and $\Delta_{1,3}$. With $\Delta^{14}C_{CO_2}$, we partitioned each measurement of CO_2 evolution into two theoretical source pools with ages of

50 yr (active-pool, $\Delta^{14}C = +146‰$) and 5,000 yr (passive-pool, $\Delta^{14}C = -360‰$). Using these partitioned CO_2 production rates, we calculated separate active-pool and passive-pool $\Delta_{1,2}$ and $\Delta_{1,3}$ values for each soil sample. As with non-partitioned data, we observed a strong linear relationship between these metrics (Fig. 3). This relationship did not differ significantly between the two pools (χ^2 (1) = 1.3042; $P = 0.2535$), indicating that active-pool and passive-pool carbon responded equivalently to the 5 °C temperature increase. After accounting for substrate depletion, we therefore found that the temperature sensitivity of decomposition was invariant across carbon pools with different cycling rates. Results were not sensitive to the specific carbon pool ages used in this analysis (Supplementary Fig. 8; Supplementary Table 5).

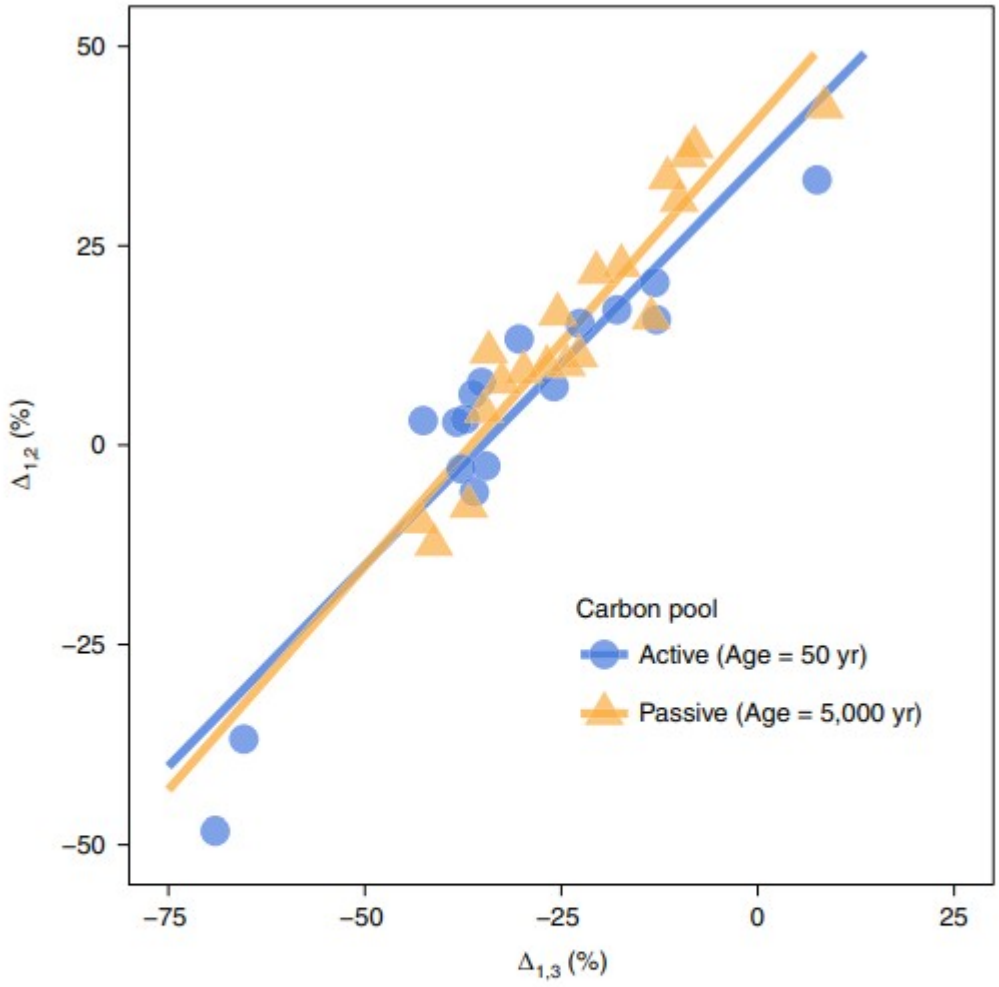

Fig. 3 | Effects of temperature and incubation time on active-pool and passive-pool CO_2 production rates. For each active-pool or passive-pool component of an incubated soil sample, $\Delta_{1,2}$ is the percentage change in CO_2 production between incubations 1 (5 °C) and 2 (10 °C), and $\Delta_{1,3}$ is the percentage change in CO_2 production between incubations 1 and 3 (both 5 °C). Regression lines represent the best linear fits, which did not differ significantly at $\alpha = 0.05$.

Our finding that slow-cycling and fast-cycling carbon were equally temperature-sensitive highlights critical differences between intrinsic temperature sensitivities of enzymatic reactions and observed temperature sensitivities of soil organic matter decomposition or enzyme activities[29,30]. In bulk soils, observed temperature sensitivities of soil organic matter decomposition integrate a range of reactions with heterogeneous intrinsic temperature sensitivities[2]. Further, biochemical and physical variables such as organo-mineral interactions, soil aggregation, interfering compounds, and

microbial constraints may limit substrate availability or inhibit enzyme function in temperature-specific ways[25], causing observed temperature sensitivities to deviate from Arrhenius predictions[2,14,29]. Finally, harsh environmental conditions may preserve otherwise unprotected carbon, minimizing differences in substrate chemistry across soil carbon age classes.

In agreement with our findings, a number of previous studies using intact (neither homogenized nor fractionated) soils found no temperature sensitivity differences among carbon pools[14,18,19,21]. By preserving soil physical structure, such studies maintained gradients of substrate availability important to the temperature response. In contrast, incubations of homogenized soils or isolated soil fractions have more often followed Arrhenius kinetics, showing increased temperature sensitivity with increased resistance to decomposition[14,16,17]. Soil homogenization may disrupt aggregation and mineral associations[13], increasing the influence of chemical recalcitrance on decomposition dynamics. Accordingly, while sieved or fractionated soils are useful for mechanistic studies[29], intact soils more closely reflect complex in situ conditions.

Our findings suggest that in these Arctic soils, ancient, historically stable carbon is readily decomposed under aerobic, thawed conditions. We find that the response of this old soil carbon to future temperature changes will not depend directly on its historical cycling rate; instead, short-term and long-term changes will probably depend on other environmental factors currently stabilizing soil carbon. This contrasts with lower-latitude sites, where fast-cycling pools dominate CO_2 production at all depths[12]. Such latitudinal differences in $\Delta^{14}C_{CO_2}$ depth profiles imply key mechanistic differences in soil organic matter preservation at depth; in Arctic soils, limited thaw days, anoxia and low fresh carbon supplies may be particularly important for deep carbon stabilization—and particularly climate-sensitive[6]. There, historically stable carbon may closely resemble more rapidly cycling substrates, rendering it highly vulnerable to soil warming, permafrost loss and active layer deepening.

Methods

Site and field sampling

Soil samples were collected from the Barrow Environmental Observatory (BEO), ~6 km east of Utqiaġvik, Alaska. Utqiaġvik has a mean annual temperature of −12 °C and mean annual precipitation of 106 mm with a short snow-free summer from June through September. Soils in the region are dominated by Typic Aquiturbels, Typic Histoturbels and Typic Aquorthels[31]. Continuous ice-rich permafrost underlies a shallow active layer, which varies in thickness from 20 to 60 cm. With low topographic relief up to 5 m elevation, the BEO ground surface consists of ice wedge polygons and drained thaw lake basins.

On 14 August 2012, we collected nine soil cores from five ice wedge polygons covering a broad range of surface vegetation, microtopography, hydrology and subsurface ice properties. Ice wedge polygons are microtopographic features ~10–30 m in diameter, separated by low-lying, wet channels called troughs. Formed by freezing and thawing of subsurface ice[32,33], polygons can be classified into three categories on the basis of subsurface ice properties and surface morphology. High-centred polygons have raised, dry centres that slope steeply into troughs, with high concentrations of subsurface ice wedges. Low-centred polygons have saturated or inundated centres and lower frequencies of subsurface ice wedges; centres are separated from troughs by raised, dry rims. Flat-centred polygons are characterized by flat surface morphology underlain by ice-rich permafrost and infrequent ice wedges; perimeter rims are not raised relative to centres[34]. Due to strong differences in physical and hydrological properties, surface vegetation and soil chemistry differ substantially among centres, rims and troughs of the three polygon types[35,36].

Soil cores were collected from centres, rims or troughs of high-centred, flat-centred and low-centred polygons (Supplementary Table 1). Cores were collected with a 1 inch diameter manual soil recovery probe to the full depth of the thawed soil layer, which ranged at the time of sampling from 21 to 39 cm across coring locations (Supplementary Table 2). Soil cores did not penetrate into permafrost. Intact cores were held at 5 °C and shipped on ice to Berkeley, CA.

Soil incubation

Six days after sampling, we divided cores into organic and mineral horizons (2–3 increments per core) and removed visible live surface vegetation and roots. Samples were otherwise left intact. We placed core increments in 8 oz glass Mason jars nested inside 32 oz glass Mason jars fitted with gastight sampling ports. Between the two jars, we added ~2 ml of deionized water to limit moisture loss from soil. To avoid artifacts from physical disturbance during core division, we pre-incubated soils for 1 d at 7.5 °C and 1 d at 5 °C before flushing jars with CO_2-free air to begin the incubation.

The experiment proceeded as three sequential incubations: 13 d at 5 °C, 16 d at 10 °C and 21 d at 5 °C. At the end of each incubation, we measured headspace CO_2 concentrations with a LI-820 CO_2 gas analyser (LI-COR) and collected headspace gas for radiocarbon analysis. Using a syringe and stopcock, we collected 30 ml of gas from each incubation jar's sampling port, then passed the sample at ~1 l min^{-1} through a septum at the inflow port of the LI-820. On the basis of repeated tests, 30 ml of gas was sufficient for a stable, accurate CO_2 concentration measurement. The remaining headspace was sampled for radiocarbon analysis using either 500 ml stainless steel sampling canisters or glass serum vials sealed with 14 mm-thick chlorobutyl septa (Bellco Glass). Following gas collection, soil was allowed to equilibrate to the new temperature for 4–7 d before jars were flushed with CO_2-free air to

begin the next incubation. At the time of sampling, headspace CO_2 concentrations ranged from 1,400 to 30,000 ppm. The percentage of initial soil carbon respired over the three short-term incubations ranged from 0.087% to 1.4% (Supplementary Table 3). To assure that jars were properly sealed, we used four blanks and four 1,000 ppm CO_2 standards throughout the incubation.

Following the third incubation, soils were freeze-dried, ground, measured into tin capsules, and analysed for carbon and nitrogen content on a Thermo Scientific Flash 2000 elemental analyser. Soil pH was measured in 0.01 M $CaCl_2$, using a 1:2 soil:solution ratio (Supplementary Table 2).

CO_2 from gas samples was cryogenically purified under vacuum, split into separate tubes for ^{14}C and ^{13}C analysis, and sealed in 6 mm quartz tubes. Subsamples of 25 ml from the 2014 incubation were composited during purification into one pair of CO_2 samples per incubation jar. For radiocarbon analysis, we sent samples to Lawrence Livermore National Laboratory's Center for Accelerator Mass Spectrometry (CAMS) or the Carbon, Water and Soils Research Laboratory at the USDA-FS Northern Research Station, where CO_2 was reduced to graphite on iron powder under H_2 (ref. 37). Abundance of ^{14}C was then measured at CAMS using a HVEC FN Tandem Van de Graaff accelerator mass spectrometer or at UC Irvine's Keck Carbon Cycle AMS facility. Analysis of $^{13}C/^{12}C$ in CO_2 splits was carried out on the UC Davis Stable Isotope Laboratory GVI Optima Stable Isotope Ratio Mass Spectrometer.

Following the conventions of Stuiver and Polach[38], radiocarbon results are presented as fractions of the modern NBS Oxalic Acid I (OX1) standard ($F^{14}C$) and as deviations in parts per thousand (‰) from the absolute (decay-corrected) OX1 standard ($\Delta^{14}C$). All radiocarbon results have been corrected for mass-dependent isotopic fractionation using ^{13}C measurements.

Data analysis

We used linear mixed-effects models to evaluate changes across the incubation periods in $\Delta^{14}C_{CO_2}$ and mean CO_2 production rates (calculated for each sample × incubation period from measured CO_2 concentrations). For each response variable—CO_2 production and $\Delta^{14}C_{CO_2}$—we constructed a linear model in which incubation number (1, 2 or 3) was the categorical fixed effect and the individual soil sample nested in soil profile was included as a random effect. This mixed model formulation accounts for baseline differences in the response variable across incubated soil samples, as well as physical clustering of soil depth increments in soil cores. *Q*–*Q* plots from these initial models showed one outlier in the CO_2 production dataset and two outliers in the $\Delta^{14}C_{CO_2}$ dataset (Supplementary Fig. 1). These outlying points were from one soil core that showed a particularly strong substrate

depletion effect between the first and second incubations. Because these outliers led to violations of model assumptions, we re-ran the above models without the outlying points. Final CO_2 production and $\Delta^{14}C_{CO_2}$ models thus represent general trends over the incubations and do not capture the full degree of potential substrate depletion. Model validation tests indicated that these final models met all model assumptions (Supplementary Fig. 3; Supplementary Fig. 4). The complete dataset was used for all other analyses and all plots.

We used radiocarbon measurements to model mean ages of carbon in the respiration flux using the method described in Vaughn and Torn[27], modified from the time-dependent steady-state model from Torn et al.[39]. Briefly, for a homogeneous carbon pool, the turnover time, defined as the inverse of the pool's cycling rate (τ), can be calculated from its measured $\Delta^{14}C$ value, the (time-dependent) $^{14}C/^{12}C$ ratio in the local atmosphere and the mean transit time of carbon through living plant material, according to:

$$F'_{C,t}C_t = IF'_{\mathrm{atm},t-T_R} + C_{t-1}F'_{C,t-1}\left(1 - \frac{1}{\tau} - \lambda\right)$$

Here, at time t, $F'_C = \frac{\Delta^{14}C}{1{,}000} - 1$ for the given carbon pool, $F'_{\mathrm{atm}} = \frac{\Delta^{14}C}{1{,}000} - 1$ for CO_2 in the local atmosphere, T_R is the mean transit time of carbon through living plant material, I is the input rate of carbon from the atmosphere to the given carbon pool, C is the stock of carbon in the given pool, and λ is the radioactive decay constant for ^{14}C (1/8,267 yr^{-1}). At steady-state, $C_t = C_{t-1} = I \times \tau$, so the above equation reduces to:

$$F'_{C,t} = \frac{1}{\tau}F'_{\mathrm{atm},t-T_R} + F'_{C,t-1}\left(1 - \frac{1}{\tau} - \lambda\right)$$

Using our measured $\Delta^{14}C_{CO_2}$ values and an annualized time series of $\Delta^{14}C$ in local atmospheric CO_2, we iteratively solved for τ. We used values from ref. 27 for atmospheric $\Delta^{14}C$, which were interpolated from refs. 40,41,42. We calculated τ twice for each sample, using T_R values of 0 and 5 yr to bracket the probable T_R range[43,44,45].

In accordance with model assumptions, we consider CO_2 production during the first incubation as an approximation of a homogeneous, steady-state system. For a homogeneous pool at steady-state, τ is equivalent to the mean

age of the carbon pool. To avoid ambiguity in terminology associated with turnover times[46], we report calculated τ values as ages of carbon being respired. When two possible carbon age solutions were obtained for a given calculation, we report both solutions.

To quantify the temperature sensitivity of decomposition, we isolated the effect of temperature on decomposition from other time-dependent changes in carbon mineralization under non-steady-state conditions (that is, substrate depletion and microbial community/activity/efficiency changes, which together we call the 'time effect'). For each incubated sample, we calculated two metrics, $\Delta_{1,2}$ and $\Delta_{1,3}$:

$$\Delta_{1,2} = \frac{J_{\mathrm{obs},2} - J_{\mathrm{obs},1}}{J_{\mathrm{obs},1}} \times 100$$

$$\Delta_{1,3} = \frac{J_{\mathrm{obs},3} - J_{\mathrm{obs},1}}{J_{\mathrm{obs},1}} \times 100$$

where $J_{\mathrm{obs},1}$, $J_{\mathrm{obs},2}$ and $J_{\mathrm{obs},3}$ are the mean CO_2 production rates during incubations 1 (5 °C), 2 (10 °C), and 3 (5 °C), respectively. Metric $\Delta_{1,2}$ quantifies the combined influences of the temperature treatment and the time effect on the decomposition rate and $\Delta_{1,3}$ quantifies the time effect alone. To isolate the temperature effect, we regressed $\Delta_{1,2}$ against $\Delta_{1,3}$ to determine whether non-steady-state effects modified the temperature response in a predictable way. This regression was performed as a linear mixed-effects model with $\Delta_{1,2}$ as the response variable, $\Delta_{1,3}$ as a fixed effect, and soil profile as a random effect. Residuals plots indicate that this analysis did not violate the assumptions of the statistical method (Supplementary Fig. 5). We found a close linear relationship between $\Delta_{1,2}$ and $\Delta_{1,3}$, which allowed us to predict the temperature response in the absence of a time effect. Specifically, the *y*-intercept of this regression (the point where the time effect equals 0) estimates the effect of a 5 °C temperature increase in the absence of source depletion or microbial acclimation.

With the y-intercept of this regression, we calculated Q_{10} using a modified form of the Van't Hoff equation:

$$Q_{10} = \left(\frac{\mathrm{intercept}}{100} + 1\right)^{\frac{10}{T_2 - T_1}}$$

where T_2 and T_1 are the temperatures at which CO_2 production rates were evaluated (5 °C and 10 °C) and $\frac{\text{intercept}}{100} + 1$ is equivalent to $\frac{R_2}{R_1}$, the ratio of CO_2 production rates at these two temperatures.

To test whether this temperature sensitivity varied among carbon pools with different cycling rates, we used radiocarbon values to partition each measurement of CO_2 evolution into fast-cycling and slow-cycling source pools. First, we defined active and passive pools with assigned ages of 50 and 5,000 yr. Corresponding to $\Delta^{14}C$ values of +146 and −360‰, these age end-members were chosen to bracket the range of observed $\Delta^{14}C$ values and represent carbon cycling on annual to decadal (active) or millennial (passive) timescales. For each incubated soil sample, we used these $\Delta^{14}C$ values in a two-pool mixing model to calculate active-pool and passive-pool contributions to CO_2 production in the three incubations:

$$\Delta^{14}C_{\text{obs},i} = f_{\text{passive},i}\,(-360‰) + f_{\text{active},i}\,(146‰)$$
$$f_{\text{passive},i} + f_{\text{active},i} = 1$$

where f_{passive} and f_{active} are the fractional contributions of the passive and active carbon pools, $\Delta^{14}C_{\text{obs}}$ is the measured $\Delta^{14}C$ value of a given CO_2 sample, and i is the incubation (1–3). We then calculated the rates of carbon mineralization from the active and passive source pools:

$$J_{\text{passive},i} = f_{\text{passive},i} \times J_{\text{obs},i}$$
$$J_{\text{active},i} = f_{\text{active},i} \times J_{\text{obs},i}$$

where J_{passive} and J_{active} are the calculated rates of CO_2 production from the passive and active pools and J_{obs} is the measured rate of CO_2 production.

Finally, with these pool-specific measurements of CO_2 production ($J_{\text{passive},i}$ and $J_{\text{active},i}$), we calculated separate active-pool and passive-pool $\Delta_{1,2}$ and $\Delta_{1,3}$ values for each incubated sample. As with non-partitioned data, we regressed $\Delta_{1,2}$ against $\Delta_{1,3}$ using a linear mixed-effects model with the response variable $\Delta_{1,2}$. This model included core increment nested in soil profile as random effects to account for paired active or passive measurements and physical clustering of increments in cores. To test whether this $\Delta_{1,2}$ versus $\Delta_{1,3}$ relationship differed between active-pool and passive-pool measurements, we used the likelihood ratio test to compare the model including $\Delta_{1,3}$ and carbon pool (active or passive) as fixed effects with the model including only $\Delta_{1,3}$ as a fixed effect. With a significance cutoff of 0.05, we found that carbon pool was not a significant predictor of $\Delta_{1,2}$ (χ^2 (1) = 1.3042; $P = 0.2535$).

We conducted a power analysis to determine the likelihood of correctly rejecting the null hypothesis at a given difference in Q_{10} between active and passive carbon pools. We evaluated the power of the likelihood ratio test at Q_{10} differences ranging from 0 to 0.2, using 400 data simulations at each Q_{10} level. In each instance, simulated $\Delta_{1,3}$ and $\Delta_{1,2}$ values were generated on the basis of characteristics of our original data, with an imposed Q_{10} difference between pools. We found the test to be highly sensitive at low differences in temperature sensitivity between pools, with a power of >0.80 for Q_{10} differences of 0.12 or greater and >0.99 for Q_{10} differences of 0.19 or greater (Supplementary Fig. 7; Supplementary Table 4).

We performed two additional analyses to evaluate the sensitivity of our findings to aspects of the analytical method. First, we repeated the CO_2 flux partitioning with passive-pool and active-pool ages of 10,000 yr ($\Delta^{14}C = -524‰$) and 20 yr ($\Delta^{14}C = +137‰$) to test whether results depended on the assigned pool structure (Supplementary Fig. 8; Supplementary Table 5). Due to the range in measured $\Delta^{14}C$ values, we could not use a passive-pool age less than ~5,000 yr or an active-pool age less than ~20 yr without reducing the set of usable data. Second, we repeated the analysis using the difference in CO_2 production between the second and third incubations to quantify the temperature effect (that is, $\Delta_{2,3} = \frac{J_{\mathrm{obs},2} - J_{\mathrm{obs},3}}{J_{\mathrm{obs},3}} \times 100$) (Supplementary Fig. 10). Findings from this test indicate that neither temperature sensitivity nor its dependence on carbon pool changed throughout the incubation.

Statistical analyses were conducted in R v.3.3.3 ‘Another Canoe’ (2017-03-06), using the packages lme4 (ref. 47) for linear mixed-effects model fitting and lmerTest[48] for significance testing. The R code developed for all analyses can be found at https://github.com/lydiajsvaughn/Radiocarbon_inc_2012.

Data availability

All data generated and analysed in this study are archived in the Next-Generation Ecosystem Experiments (NGEE-Arctic) data repository[49] and can be accessed at https://doi.org/10.5440/1418852.

References

1. Koven, C. D. et al. Permafrost carbon-climate feedbacks accelerate global warming. Proc. Natl Acad. Sci. USA 108, 14769–14774 (2011). 2. Davidson, E. A. & Janssens, I. A. Temperature sensitivity of soil carbon decomposition and feedbacks to climate change. Nature 440, 165–173 (2006). 3. Koven, C. D., Lawrence, D. M. & Riley, W. J. Permafrost carbon−climate feedback is sensitive to deep soil carbon decomposability but not deep soil nitrogen dynamics. Proc. Natl Acad. Sci. USA 112, 3752–3757 (2015). 4. Knorr, W., Prentice, I. C., House, J. I. & Holland, E. A. Long-term sensitivity of soil carbon turnover to warming. Nature 433, 298–301 (2005). 5. Hugelius, G. et al. Estimated stocks of circumpolar permafrost carbon with quantifed

uncertainty ranges and identifed data gaps. Biogeosciences 11, 6573–6593 (2014). 6. Schuur, Ea. G. et al. Climate change and the permafrost carbon feedback. Nature 520, 171–179 (2015). 7. Jorgenson, M. T., Shur, Y. L. & Pullman, E. R. Abrupt increase in permafrost degradation in Arctic Alaska. Geophys. Res. Lett. 33, L02503 (2006). 8. Osterkamp, T. E. & Romanovsky, V. E. Evidence for warming and thawing of discontinuous permafrost in Alaska. Permafr. Periglac. Process. 10, 17–37 (1999). 9. Schuur, E. A. et al. Te efect of permafrost thaw on old carbon release and net carbon exchange from tundra. Nature 459, 556–559 (2009). 10. Hicks Pries, C. E., Schuur, E. A. G. & Crummer, K. G. Tawing permafrost increases old soil and autotrophic respiration in tundra: partitioning ecosystem respiration using δC and Δ14C. Glob. Change Biol. 19, 649–661 (2013). 11. Jones, C. D., Cox, P. & Huntingford, C. Uncertainty in climate–carbon-cycle projections associated with the sensitivity of soil respiration to temperature. Tellus B 55, 642–648 (2003). 12. Trumbore, S. Age of soil organic matter and soil respiration: radiocarbon constraints on belowground C dynamics. Ecol. Appl. 10, 399–411 (2000). 13. Lützow, Mv et al. Stabilization of organic matter in temperate soils: mechanisms and their relevance under diferent soil conditions—a review. Eur. J. Soil Sci. 57, 426–445 (2006). 14. Conant, R. T. et al. Temperature and soil organic matter decomposition rates – synthesis of current knowledge and a way forward. Glob. Change Biol. 17, 3392–3404 (2011). 15. Hartley, I. P. & Ineson, P. Substrate quality and the temperature sensitivity of soil organic matter decomposition. Soil Biol. Biochem. 40, 1567–1574 (2008). 16. Craine, J. M., Fierer, N. & McLauchlan, K. K. Widespread coupling between the rate and temperature sensitivity of organic matter decay. Nat. Geosci. 3, 854–857 (2010). 17. Feng, X. & Simpson, M. J. Temperature responses of individual soil organic matter components. J. Geophys. Res. Biogeosci. 113, G03036 (2008). 18. Townsend, A. R., Vitousek, P. M., Desmarais, D. J. & Tarpe, A. Soil carbon pool structure and temperature sensitivity inferred using CO2 and 13CO2 incubation fuxes from fve Hawaiian soils. Biogeochemistry 38, 1–17 (1997). 19. Fang, C., Smith, P., Moncrief, J. B. & Smith, J. U. Similar response of labile and resistant soil organic matter pools to changes in temperature. Nature 433, 57–59 (2005). 20. Gillabel, J., Cebrian-Lopez, B., Six, J. & Merckx, R. Experimental evidence for the attenuating efect of SOM protection on temperature sensitivity of SOM decomposition. Glob. Change Biol. 16, 2789–2798 (2010). 21. Dioumaeva, I. et al. Decomposition of peat from upland boreal forest: temperature dependence and sources of respired carbon. J. Geophys. Res. Atmos. 107, 8222 (2002). 22. Kleber, M. et al. Old and stable soil organic matter is not necessarily chemically recalcitrant: implications for modeling concepts and temperature sensitivity. Glob. Change Biol. 17, 1097–1107 (2011). 23. Reichstein, M. et al. Temperature sensitivity of decomposition in relation to soil organic matter pools: critique and outlook. Biogeosciences 2, 317–321 (2005). 24. Bradford, M. A. et al. Termal adaptation of soil microbial respiration to elevated temperature. Ecol. Lett. 11, 1316–1327 (2008). 25. Tang, J. & Riley, W. J. Weaker soil carbon–climate feedbacks resulting from

microbial and abiotic interactions. Nat. Clim. Change 5, 56–60 (2015). 26. Lupascu, M., Welker, J. M., Xu, X. & Czimczik, C. I. Rates and radiocarbon content of summer ecosystem respiration in response to long-term deeper snow in the High Arctic of NW Greenland. J. Geophys. Res. Biogeosci. 119, 2013JG002494 (2014). 27. Vaughn, L. J. S. & Torn, M. S. Radiocarbon measurements of ecosystem respiration and soil pore-space CO2 in Utqiaġvik (Barrow), Alaska. Earth Syst. Sci. Data. 10, 1943–1957 (2018). 28. Friedlingstein, P. et al. Climate–carbon cycle feedback analysis: results from the C4MIP model intercomparison. J. Clim. 19, 3337–3353 (2006). 29. German, D. P., Marcelo, K. R. B., Stone, M. M. & Allison, S. D. Te Michaelis–Menten kinetics of soil extracellular enzymes in response to temperature: a cross-latitudinal study. Glob. Change Biol. 18, 1468–1479 (2012). 30. Min, K., Lehmeier, C. A., Ballantyne, F., Tatarko, A. & Billings, S. A. Diferential efects of pH on temperature sensitivity of organic carbon and nitrogen decay. Soil Biol. Biochem. 76, 193–200 (2014).

Acknowledgements

This research was conducted through the Next-Generation Ecosystem Experiments (NGEE-Arctic) project, which is supported by the Office of Biological and Environmental Research in the US Department of Energy Office of Science.